An EXAFS study of thermal disorder in GaAs



1994 J. Phys.: Condens. Matter 6 3599

(http://iopscience.iop.org/0953-8984/6/19/016)

J. Phys.. Condens. Matter 6 (1994) 3599–3608. Printed in the UK

# An EXAFS study of thermal disorder in GaAs

G Dalba†, D Diop†§, P Fornasini† and F Rocca‡

† Dipartimento di Fisica, Università di Trento, I-38050 Povo (Trento), Italy

‡ Centro di Fisica degli Stati Aggregati ed Impianto Ionico del Consiglio Nazionale delle Ricerche e Istituto Trentino di Cultura, I-38050 Povo (Trento), Italy

Received 6 August 1993, in final form 12 January 1994

**Abstract.** This paper presents the experimental results of a cumulant analysis of the extended x-ray absorption fine structure amplitude of GaAs at the K edges of Ga and As. The second and fourth cumulants of the distance distributions of the near neighbours of Ga and As have been obtained as a function of temperature in the range 77–450 K. The fourth cumulant of Ga–As nearest-neighbour distance distributions is zero in the examined temperature range; a non-Gaussian distribution of the second and third coordination shell distances of Ga and As has been revealed for the first time. Temperature dependences of mean square relative displacements (MSRDs) of the first three shells of Ga and As have been compared with Einstein and correlated Debye models. The MSRD of the first-shell Ga–As distance is connected to the optical modes at 7.6–8 THz of the phonon spectrum of GaAs.

## 1. Introduction

The potential of extended x-ray absorption fine structure (EXAFS) as a vibrational probe, recognized since the seventies by many authors [1–3], is now being exploited to study the vibrational properties of a great many crystalline materials. The temperature dependence of the EXAFS Debye–Waller factors, analysed in harmonic approximation, has allowed extraction of information on nearest-neighbour force constants in molecular crystals [4] as well as to investigate the existence of anomalies of phonon modes in superconducting materials [5]. The damping of EXAFS amplitude with increasing temperature comes from the thermal broadening of the distribution of distances. Asymmetric distributions of distances due to moderate thermal and static disorder are studied by the expansion of EXAFS amplitude and phase in terms of cumulants [6–8]; these analyses are now producing interesting results [9–11]. The cumulant temperature dependence of the cumulants gives information on the local vibrational properties and the extent of the distribution asymmetry.

In this work we present the second and fourth cumulants of the distance distributions for the first three coordination shells of Ga and As in GaAs in the temperature range 77–450 K.

The second cumulant of the distance distributions corresponds to the mean square relative displacement (MSRD) of atomic pairs. MSRD is the sum of two contributions: the mean square displacement (MSD) of the elements of the atomic pair and the displacement correlation function (DCF) between them [1]. The MSD can be obtained from the thermal factor of x-ray or neutron diffraction [12]. Unfortunately the available experimental data on MSD are often scarce and sometimes unreliable as in the case of GaAs [13]; calculations of atomic displacements based on refined force constant models have been carried out for

§ On leave from the Department of Physics of the University of Dakar, Senegal.

0953-8984/94/193599+10$19.50  

GaAs in the harmonic approximation [12, 14]. As for the GaAs MSRD, only a few EXAFS experimental data have been published [15].

The MSRD and MSD contain information about phonon eigenvectors not directly obtainable with most other techniques. MSRD, compared with MSD, is sensitive not only to the modulus of eigenvectors but also to the phase relationships of central and backscattering atoms, although, for unpolarized measurements, it is insensitive to the absolute direction of eigenvectors. MSRD and MSD measurements as a function of temperature can constitute valid probes of vibrational dynamics of polyatomic crystals. The comparison of MSRD and MSD in GaAs allows us to show the degree of correlation in atomic motion for the first three coordination shells of Ga and As.

For the first time, thanks to the treatment of EXAFS in terms of cumulants, the asymmetry of the distance distributions in the outer coordination shells around a given absorbing species is shown.

In section 2 we review the basic principles of the cumulant method; in section 3 we illustrate the data analysis procedure; in section 4 we present the experimental data and compare them with other data and theoretical models. In section 5 we discuss the MSRD results. Final remarks are made in section 6.

## 2. Expansion of EXAFS in cumulant series

In the single-electron single-scattering and plane wave approximation the EXAFS interference function $\chi_j(k)$, relative to the $j$th coordination shell of a selected species of a polycrystalline or amorphous sample, is given by

$$\chi_j(k) = \frac{S_0^2}{k} N_j \operatorname{Im}\left\{ F_j(k) e^{2i\delta_l} \int_0^\infty P_j(r,\lambda) e^{2ikr} dr \right\} \tag{1}$$

where $S_0^2$ takes into account the intrinsic inelastic effects, $k$ is the photoelectron wavevector, $N_j$ the coordination number, $F_j$ the backscattering amplitude and $\delta_l$ the central atom phaseshift. $P_j(r,\lambda)$ is the effective distribution of atomic positions $r$ of the backscattering atoms relative to the central atom:

$$P_j(r,\lambda) = \rho_j(r) \frac{1}{r^2} e^{-2r/\lambda}$$

with $\rho_j(r)$ representing the real distribution and $\lambda$ the mean free path of photoelectrons; in crystalline compounds, for an undistorted coordination shell, the width of $\rho_j(r)$ is due only to the thermal disorder. The integral in equation (1) is the characteristic function of the effective distribution. The logarithm of the characteristic function can be developed in MacLaurin series [7] around $k = 0$

$$\ln \int_0^\infty P_j(r,\lambda) e^{2ikr} dr = \sum_{n=0}^{\infty} \frac{(2ik)^n}{n!} C_{nj}. \tag{2}$$

$C_{nj}$ are the cumulants of the effective distribution.

From equations (1) and (2), by truncating the cumulant series at the fourth term, the EXAFS of the $j$th shell can be factorized as

$$\chi_j(k) = A_j(k) \sin \phi_j(k). \tag{3}$$

The amplitudes $A_j(k)$ and phases $\phi_j(k)$ can be expressed as

$$A_j(k) = \frac{S_0^2 N_j}{k} |F_j(k)| \exp(C_{0j}) \exp\left( -2C_{2j}k^2 + \frac{2}{3} C_{4j} k^4 + \dots \right) \tag{4}$$

$$\phi_j(k) = 2kC_{1j} - \frac{4}{3}C_{3j}k^3 + \ldots + \varphi_j(k) \tag{5}$$

where $\varphi_j$ is the total photoelectron phaseshift. Equations (4) and (5) contain the cumulants $C_{nj}$ of the effective distribution of the distances $P_j(r, \lambda)$. The connection to the cumulants of the real distribution $\rho_j(r)$ is obtained through approximated series expansion of the characteristic function [6–8, 16]. In particular the average value $R_j$ of $\rho_j(r)$ is related to $C_{1j}$ and $C_{2j}$ by the relation

$$C_{1j} = R_j - \frac{2C_{2j}}{R_j}\left(1 + \frac{R_j}{\lambda}\right).$$

As for cumulants of order higher than unity, the difference between real and effective distribution is generally considered negligible with respect to the experimental uncertainty. For not too large distributions, the normalization factor in equation (4) is approximated as: $\exp(C_{0j}) = \exp(-2R_j/\lambda)/R_j^2$ [6].

Tests on model distributions representing moderately disordered systems have shown that the first four cumulants are enough to adequately reproduce the original distributions [17]. In the case of GaAs the higher cumulant terms have been proved to be important only for the outer shell analysis.

In terms of the atomic displacements $u_0$ and $u_j$ of central and backscattering atoms, the cumulants $C_{nj}$ can be expressed as

$$C_{nj} = \langle[(u_j - u_0) \cdot \hat{r}_j]^n\rangle \tag{6}$$

where $\hat{r}_j = r_j/r_j$, and $r_j$ is the atomic vector position in the $j$th shell [8]. For harmonic Hamiltonians the cumulants higher than two are equal to zero.

The second cumulant $C_{2j}$ coincides with the MSRD

$$C_{2j} = \langle[(u_j - u_0) \cdot \hat{r}_j]^2\rangle = \text{MSRD} \tag{7}$$

(for disordered systems MSRD contains anharmonic contributions).

By developing the product in square brackets it emerges that

$$C_{2j} = \langle(u_0 \cdot \hat{r}_j)^2\rangle + \langle(u_j \cdot \hat{r}_j)^2\rangle - 2\langle(u_0 \cdot \hat{r}_j)(u_j \cdot \hat{r}_j)\rangle. \tag{8}$$

So, the MSRD is the difference between the sum of the MSD of the central $\langle(u_0 \cdot \hat{r}_j)^2\rangle$ and backscattering atoms $\langle(u_j \cdot \hat{r}_j)^2\rangle$ and the DCF $2\langle(u_0 \cdot \hat{r}_j)(u_j \cdot \hat{r}_j)\rangle$.

## 3. Experimental details and data analysis procedure

The x-ray absorption spectra of Ga and As K edges were recorded in transmission mode at the synchrotron radiation facilities, PWA BX-2 and PULS, of Adone storage ring (Frascati, Italy). The electron energy was 1.5 GeV, the wiggler magnetic field 1.6 T and the maximum stored current 60 mA. A (220) silicon channel-cut crystal monochromator was utilized. The total energy resolution was estimated to be $\Delta E \simeq 1$ eV at 10 keV.

The sample was prepared from a GaAs monocrystal which was finely ground in grains with size lower than 10 $\mu$m; the powder was uniformly deposited on a polytetrafluoroethylene membrane by a sonication method. Samples with different thicknesses were measured to check for the 'thickness effect' which can result because of sample inhomogeneity. An edge step $\Delta(\mu x) \simeq 1$ at Ga and As K edges was considered.

A liquid nitrogen cryostat was used to adjust the sample temperature $T$ within an uncertainty of $\pm 2$ K; nine points at different temperatures were recorded in the range 77–450 K.

The EXAFS modulation $\chi(k)$ has been extracted from the experimental absorption coefficient $\mu(E)$ at Ga and As K edges following the conventional procedure [18]. The photoelectron wavevector $k$ has been derived from the photon energy $E$ by the formula $k^2 = 2m/\hbar^2(E - E_0)$ where $E_0$ has been set at the maximum of the first derivative of the absorption spectrum and $m$ is the electron mass. Figure 1 (left) shows the EXAFS signal $k\chi(k)$ for two selected temperatures. The amplitude reduction of the EXAFS signal is due to the thermal disorder. The $\chi(k)$ spectra, ranging from 3.5 to 14.5 $\text{Å}^{-1}$ and weighted by $k^3$, were Fourier transformed in the space of interatomic distances $R$ using a square window. The modulus of the Fourier transform of $k^3\chi(k)$ is shown in figure 1 (right): the peaks relative to the first three shells are well defined and separated. EXAFS single-shell contributions were obtained by back-transforming each peak to the $k$ space. Experimental single shell amplitude and phase functions, $A_j(k)$ and $\phi_j(k)$, have been obtained from the real and imaginary parts of the filtered signals $\chi_j(k)$. Structural information has been extracted from the EXAFS formula (equation (3)); in the following we analyse only the amplitude functions (equation (4)); data of comparable reliability could not be obtained from phase analysis. The EXAFS analysis beyond the first shell has been possible for the negligible contribution of multiple scattering under the second- and third-shell peaks as we have shown in a previous calculation [19].

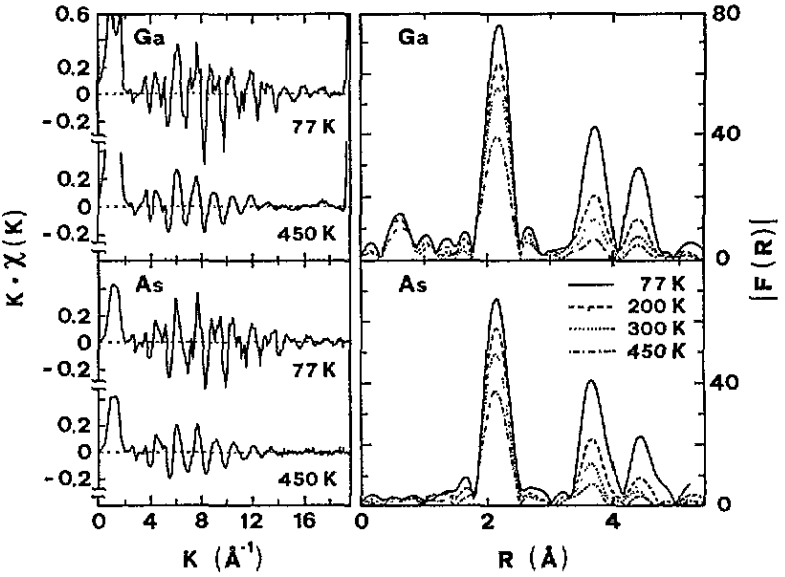


Figure 1. $k\chi(k)$ EXAFS signals (left) at the Ga and As K edges, and the moduli of Fourier Transforms (right) at selected temperatures.

The amplitude analysis was carried out using the ratio method [11, 17] which allows the extraction of thermal parameters $C_{2j}$ and $C_{4j}$ relative to a reference temperature. Single-shell experimental amplitudes at a given temperature $T$, $A(T)$, have been compared with the corresponding amplitude at 77 K, $A(77K)$, through the formula

$$\ln\frac{A_j(T)}{A_j(77K)} = \ln\frac{N_j R_{jr}^2}{N_{jr} R_j^2} - 2\frac{\Delta R_j}{\lambda} - 2k^2\Delta C_{2j} + \frac{2}{3}k^4\Delta C_{4j}$$

where $\Delta C_{2j} = C_{2j}(T) - C_{2j}(77K)$ and $\Delta C_{4j} = C_{4j}(T) - C_{4j}(77K)$ refer to the second and fourth cumulants of the $j$th shell and the index r indicates the reference parameters at 77 K.

We have assumed $N_j/N_{jr} = 1$ and $\Delta R_j = 0$, that is, we have used the crystallographic coordination numbers for the first three shells of Ga and As and neglected the effect of thermal expansion on bond lengths in the examined temperature range. The temperature independent factors influencing $A_j(T)$ present in equation (5) have been considered to be equal to the ones of the reference spectra at 77 K. The logarithm of the amplitude ratio versus $k^2$ is shown in figure 2, for the first three coordination shells of As; similar curves have been obtained for the three shells of Ga. While for the first shell (figure 2 left) the curves appear linear in the whole temperature range, they progressively deviate from linearity with temperature for the second and third shells (figure 2 centre and 2 right); a non-linear behaviour of the logarithm of the amplitude ratio as a function of $k^2$ is a sign of a non-Gaussian distribution. $\Delta C_{2j}(T)$ and $\Delta C_{4j}(T)$ have been obtained by fitting a polynomial $\alpha_2 k^2 + \alpha_4 k^4$ to the experimental curves in figure 2. The polynomial coefficients of the fitting procedure constitute a good approximation to the exact cumulants when the cumulant series is rapidly convergent [17]. This is true for moderately disordered systems such as GaAs in the examined temperature range.

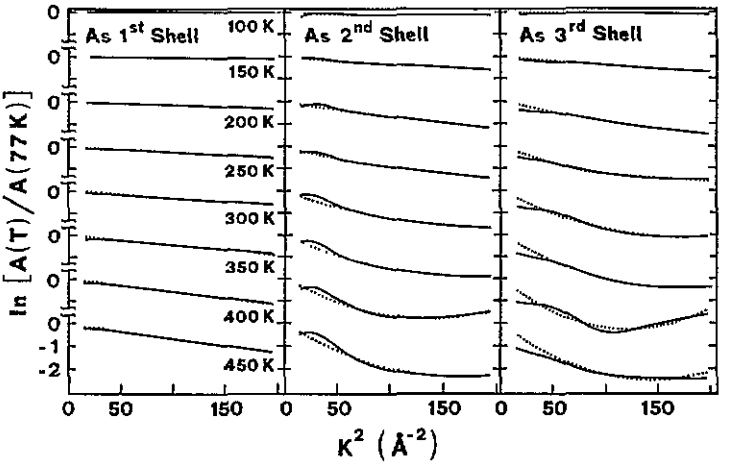


**Figure 2.** The logarithm of the EXAFS amplitude ratio functions versus $k^2$ (continuous lines) for the first (left), second (centre) and third (right) coordination shells of As in GaAs; second order polynomial fitting curves (dashed lines). The best fit has been done in the range 5-14 Å .

## 4. Results

The experimental results of $\Delta C_{2j}(T)$ and $\Delta C_{4j}(T)$ have been extracted from three sets of EXAFS measurements at each temperature. Casual errors have been found to be negligible with respect to systematic errors coming from different data analysis. By changing the procedure of background subtraction and the parameters of Fourier and back-Fourier transforms, the overall uncertainties of $\Delta C_{2j}$ have been evaluated to be less than $\pm 10\%$ for the first and second shells and about $\pm 15\%$ for the third shells (figure 3) [20]; the uncertainties of $\Delta C_{4j}$ are about 20% (figure 4).

In table 1, the values of $\Delta C_{2j}$ at room temperature are compared with the only experimental [21] and theoretical [16] data available in the literature. The differences between the experimental results may be due to different data analysis; as a matter of fact we have verified that the use of a standard procedure, which assumes a Gaussian disorder,

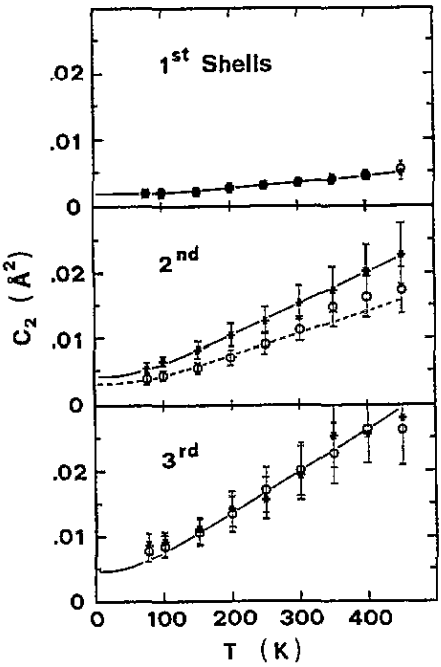


Figure 3. Second cumulant (Mean Square Relative Displacement) of the first three coordination shells of As (circles) and Ga (asterisks) in GaAs as a function of temperature. The lines are Einstein models.

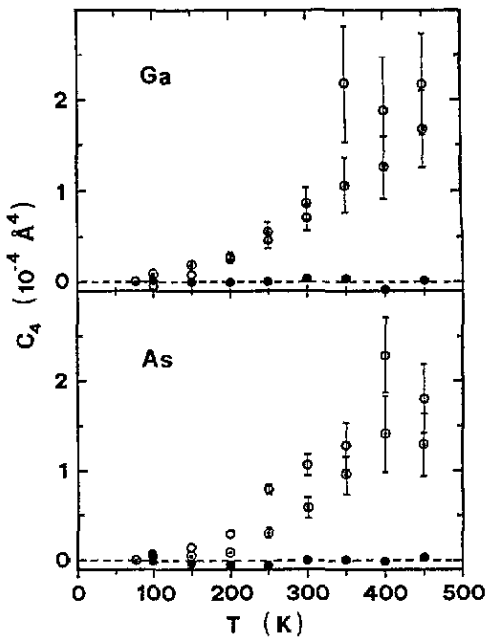


Figure 4. Fourth cumulants $C_4$ of the distance distribution for the first (solid circles), second (dotted circles) and third (open circles) coordination shells of As and Ga in GaAs.

Table 1. Difference $\Delta C_2 = C_2(295\ \text{K}) - C_2(77\ \text{K})$ (in $10^{-2}$ Å$^2$) between the second cumulants $C_2$ at 295 and 77 K for the first- and second-shell distances in GaAs.

| References | Ga–As First shell | Ga–Ga Second shell | As–As Second shell |
|---|---|---|---|
| Present work | 0.15±0.01 | 0.99±0.08 | 0.75±0.06 |
| [21] | 0.21±0.01 | 0.71±0.14 | 0.56±0.11 |
| [16] | 0.173 | 0.755 | 0.662 |

can significantly affect the $\Delta C_{2j}$ values. The discrepancy between our experimental data and theoretical data is mainly due to the anharmonic contribution present in the experimental $\Delta C_{2j}$ which is not taken into account in the lattice dynamical calculation. In any case all data in table 1 agree in the fact that Ga–Ga $\Delta C_2$ is larger than As–As $\Delta C_2$, while, according to some calculations [12] the Ga MSD is smaller than the As MSD. This can be explained by the difference in the correlation between the motion of Ga–Ga and As–As pairs.

The fitting procedure of the logarithm of amplitude ratio, based on comparison with a reference, yields relative values $\Delta C_{2j}(T)$ and $\Delta C_{4j}(T)$. The absolute values of $C_{2j}$ for the first three shells of Ga and As are shown in figure 3 as a function of temperature. They have been obtained by vertically shifting the experimental points to match the Einstein model curve (continuous line) which best fits the slope of experimental data at high temperatures. The absolute values of $C_{4j}$ reported in figure 4 have been obtained by hypothesizing a

Gaussian behaviour at 77 K.

In figure 3 it is evident that the second cumulants $C_{2j}$ increase with temperature and distance from the central atoms (Ga or As), but for the first shell the fourth cumulant $C_4$ is zero (figure 4, solid circles) in the whole temperature range, for the second shell Ga–Ga and As–As and the third shell Ga–As distances it increases with temperature (figure 4, dotted and empty circles). This fact suggests that, in the examined temperature range, the distribution of distances of the first shell is Gaussian while the outer-shell distributions are not Gaussian; values $C_4 > 0$ are typical of distributions with a shape narrow in the centre and wide and flat on the wings. So, the weaker the bonding of backscattering atoms to the central atom, the wider and more non-Gaussian the distributions become. Cubic polynomials have been best fitted to the $C_{4j}$ in figure 4 since a behaviour of the form $A_4T^3$ is expected in the case of moderate thermal disorder [22]. $A_4$ is zero for the first shell, is equal to $2.19\times10^{-12}$ and $2.3\times10^{-12}$ (Å$^4$ K$^{-3}$) for the Ga–Ga and As–As distances of the second shells and to $3.18\times10^{-12}$ (Å$^4$ K$^{-3}$) for the third-shell distances Ga–As.

## 5. Discussion.

We will focus our attention on the temperature dependence of the second cumulant. The difference between MSRD and MSD is given by the DCF (equation (6)). Figure 5 shows the MSRD of the first three shells of Ga and As together with the theoretical MSD $\langle u_{Ga}^2\rangle + \langle u_{As}^2\rangle$ (crosses in figure 5) calculated by Reid [12] according to a shell model. From figure 5 it is evident that the correlation of motion between central and backscattering atoms, very strong for the first shell, decreases for the outer shells, becoming almost negligible already in the third shell. However, since the force constant models are calculated in the harmonic approximation, a correct comparison with experimental results can be made only after the subtraction of the anharmonic contribution from the experimental MSRD of the second and third shells. This subtraction can be done if all four cumulants are known as it has been shown in the case of crystalline Ge [23]. In the case of Ge, which has structural properties and cumulants $C_2$, $C_4$ very close to those of GaAs, the anharmonic contribution amounts to about 5–8% of the MSRD of the second and third shells.

**Table 2.** Frequencies (THz) and temperatures (K) of the Einstein and Debye models for $\sigma^2$ of Ga and As first three shells distances.

| | | Einstein model | | Debye model | |
|---|---|---|---|---|---|
| Central atom | Shells | Frequency (THz) | Temperature (K) | Frequency (THz) | Temperature ( K) |
| Ga | First, Ga–As | 7.5±0.5 | 360 | 9.0±0.6 | 430 |
| | Second, Ga–Ga | 3.5±0.4 | 170 | 5.3±0.5 | 255 |
| | Third, Ga–As | 3.0±0.3 | 155 | 4.8±0.5 | 230 |
| As | First, As-Ga | 7.5±0.5 | 360 | 9.0±0.6 | 430 |
| | Second, As–As | 4.0±0.4 | 195 | 5.8±0.5 | 280 |
| | Third, As-Ga | 3.0±0.3 | 155 | 4.8±0.5 | 230 |

The Einstein and Debye models are often used to calculate the temperature dependence of the MSRD in the absence of knowledge of the microscopic force constants [3, 8]. In principle the Einstein model seems appropriate when vibrational modes giving the prominent contribution to relative motion fall in a narrow energy band; the correlated Debye model

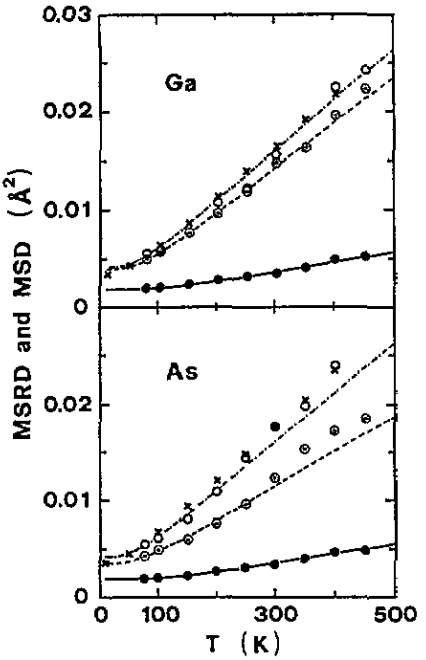


**Figure 5.** Uncorrelated MSD $\langle u^2_{Ga}\rangle + \langle u^2_{As}\rangle$ from [11] (crosses) and MSRD for the first (solid circles), second (dotted circles) and third (open circles) coordination shells of As and Ga in GaAs.

gives a better approximation when a wider range of modes is important. In table 2 the frequencies and temperatures of the Einstein models which best fit the experimental data are reported for the three shells of Ga and As: it is noteworthy that the Ga–Ga second-shell frequency is lower than the As–As one, and that the first- and third-shell Ga–As Einstein frequencies extracted from the Ga K edge coincide, within the experimental accuracy, with the ones extracted from the As K edge. The Einstein frequencies reported in table 2 constitute useful information about the strength of the effective bond stretching forces. The effective stretching force constants of the first, second and third shells are reported in table 3. In general the Einstein frequencies cannot be correlated in a simple way to the phonon density of states. For GaAs the total phonon density of states is characterized by a broad band of modes centred at about 2 THz, associated with TA modes, by smaller peaks near 5.7 and 6.8 THz due to LA modes and by a sharp peak centred at about 7.6–8 THz from a massive concentration of optical modes [24, 25]. Since the low frequency acoustic modes yield a strong correlation of atomic motion they cannot significantly influence the first-shell MSRD; it is thus reasonable to assume that the first-shell Ga–As bonding ($\nu_E$ = 7.50 THz) is mainly influenced by the high-frequency optical modes. The same conclusion was attained by other authors [8] for crystalline Ge which is characterized by a density of vibrational modes very similar to the one of GaAs.

**Table 3.** *Effective stretching force constants derived from Einstein frequencies in table 2.*

| Shell | Bond | $k$ (N m$^{-1}$) |
|---|---|---|
| First | Ga–As | 133 |
| Second | Ga–Ga | 28 |
| Second | As–As | 39 |
| Third | Ga–As | 21 |

We have also tried to fit the experimental MSRD with a correlated Debye model [1]. For cubic monatomic crystals the Debye approximation is most suitable since it takes into account only the acoustic branches of the phonon dispersion curves. The application of Debye theory to polyatomic crystals, with a basis of $p$ atoms per lattice point, has been reviewed for x-ray diffraction by Horning and Staudenmann [26]. In such solids the $3p$ branches can be represented in a single Brillouin zone, the so called reduced zone or, equivalently, in an extended zone which consists of $p$ zones each containing three branches. In both representations acoustic and optical branches are substituted by constant-velocity acoustic branches. Horning and Staudenmann have shown that, in the classic limit, the specific heat Debye temperature, $\theta_D$, and the x-ray Debye temperature, $\theta_M$, are related by $\theta_D = \theta_M p^{1/2}$; for GaAs they report $\theta_D = 355$ K and $\theta_M = 247$ K. $\theta_M$ represents a measure of the mean square atomic displacements. EXAFS is sensitive to the relative displacements between central and backscattering atoms, so a Debye model must deal with correlated motion as Beni and Platzman showed [1]. We have calculated the MSRD of Ga and As coordination shells (equation (8) in [27]) using the Debye temperature as free parameter of the correlated Debye model which best fits the slope of experimental curves. The calculations have been done for the extended zone characterized by a Debye wavevector $q_D = 1.38$ Å$^{-1}$; Debye frequencies ($\omega_D = k_B\theta_D/\hbar$) and temperatures are reported in table 2. In the third shell, where the correlated motion is reduced, the EXAFS Debye temperature $\theta_D = 230$ K is close to the x-ray diffraction $\theta_M = 245$ K. As shown in table 2 the Debye correlated model is not adequate to interpret the MSRD temperature dependence of the first three shell distances with only one temperature [1]. The inadequacy is due to a wrong evaluation of atomic correlation and to the fact that the atomic relative displacements in each shell are influenced by different parts of the phonon spectrum. EXAFS Debye temperatures can represent measurements of the MSRD. However more significant physical parameters can be obtained by comparing the experimental MSRD with refined force constant models or *ab initio* methods.

## 6. Conclusions.

We have measured EXAFS at the K edges of Ga and As in GaAs in the temperature range 77–450 K. Analysing the EXAFS amplitude in terms of cumulants, we have determined the temperature dependence of the second and fourth cumulants of the distance distributions for the first three coordination shells of Ga and As. A harmonic behaviour has been found for the first shell. For the first time a non-Gaussian distribution of distances in the outer shells has been monitored by the fourth cumulant.

A comparison of MSRD of the first three shells of Ga and As with MSD shows that the extent of correlation of the atomic motion in the three shells strongly decreases with increasing the interatomic distance. This effect is accounted for by the phase relationships of phonon eigenvectors; the effect is relevant in non-Bravais lattices due to the influence of optical branches [27]. The simplest approximated dynamical calculation, i.e. the Einstein model, has allowed to extract the effective stretching force constants of the Ga and As bonding in the first three shells. Different Debye temperatures are required to interpret experimental MSRD by the correlated Debye model. The inadequacy of the Debye approximation, typical of crystals with a strong covalent bonding character [2], shows that the interpretation of correlation in the various shells requires more realistic models. Recent GaAs vibrational dynamics calculations based on many refined force constant models have been reported by Strauch and Dorner [14]. The sensitivity of MSRD to the phonon polarization could represent a useful test of these models.

**Acknowledgments**

We thank Professor E Burattini, Professor S Mobilio and the staff of the Synchrotron Radiation facilities of the Frascati National Laboratories for their collaboration. The support of Dr P Maistrelli in the preliminary characterization of samples by x-ray diffraction is gratefully acknowledged.

## References

[1] Beni G and Platzman P M 1976 *Phys. Rev.* B **14** 1514
[2] Böhmer W and Rabe P 1979 *J. Phys. C: Solid State Phys.* **12** 2465
[3] Sevillano E, Meuth H and Rehr J 1979 *Phys. Rev.* B **20** 4908
[4] Tranquada J M and Yang C Y 1987 *Solid State Commun.* **63** 211
[5] Tranquada J M, Heald S H and Moodenbaugh A R 1987 *Phys. Rev.* B **36** 8401
[6] Freund J, Ingalls R and Crozier E D 1989 *Phys. Rev.* B **39** 12537
[7] Bunker G 1983 *Nucl. Instrum. Methods* **207** 437
[8] Crozier E D, Rehr J J and Ingalls R 1988 *X-ray Absorption* ed D C Koningsberger and R Prins (New York: Wiley) p 373
[9] Stern E A, Ma Y, Hanske-Petitpierre O 1992 *Phys. Rev.* B **46** 687
[10] Wenzel L, Arvanitis D, Rabus R, Lederer T and Baberske K 1990 *Phys. Rev. Lett.* **64** 1765
[11] Stern E A, Ma Y, Hanske-Petitpierre O and Bouldin C E 1992 *Phys. Rev.* B **46** 687
[12] Reid J S 1982 *Acta Crystallogr.* A **39** 1
[13] Matsushita T and Hayashi J 1977 *Phys. Status. Solidi* a **41** 139
[14] Strauch D and Dorner B 1990 *J.Phys.: Condensed Matter* **2** 1457
[15] Theye M L, Gheorghiu A and Launois H 1980 *J. Phys. C: Solid State Phys.* **13** 6569
[16] Tranquada J M 1983 *PhD Thesis* Washington University
[17] Dalba G, Fornasini P and Rocca F 1993 *Phys. Rev.* B **47** 8502
[18] Lee P A, Citrin P H, Eisenberger P and Kinkaid B M 1981 *Rev. Mod. Phys.* **53** 769
[19] Dalba G, Diop D, Fornasini P, Kuzmin A and Rocca F 1993 *J. Phys.: Condens. Matter* **5** 1643
[20] Burattini E, Dalba G, Diop D, Fornasini P and Rocca F 1993 *Japan. J. Appl. Phys.* **32** 89
[21] Stern E A, Bunker G and Heald S M 1980 *Phys. Rev.* B **21** 5521
[22] Tranquada J M and Ingalls R 1983 *Phys. Rev.* B **28** 3520
[23] Dalba G, Fornasini P, Grazioli M and Rocca F (to be published)
[24] Besson J M, Itiè J P, Polian A, Weill G, Mansot J L and Gonzales J 1991 *Phys. Rev.* B **44** 4214
[25] Blakemore J S 1982 *J. Appl. Phys.* **53** R123
[26] Horning R D and Staudenmann J L 1988 *Acta Crystallogr.* A44 136
[27] Dalba G, Fornasini P, Rocca F and Mobilio S 1990 *Phys. Rev.* B **41** 9668